Ocean Science
Discussions

Water exchange between the Sea of Azov and the Black Sea through the Kerch Strait

Ivan Zavialov[1], Alexander Osadchiev[1]

[1]Shirshov Institute of Oceanology, Russian Academy of Sciences, Moscow, Russia.

5   *Correspondence to*: Alexander Osadchiev (osadchiev@ocean.ru)

Abstract. The Sea of Azov is a small, shallow and freshened sea that receives a large freshwater discharge and, therefore, can be regarded as a large river estuary. Under certain external forcing conditions low-saline waters from the Sea of Azov inflow to the northeastern part of the Black Sea through the narrow Kerch Strait and form a surface-advected buoyant plume. Water flow in the Kerch Strait also regularly occurs in the opposite direction, which results in spreading of a bottom-

10   advected plume of saline and dense waters from the Black Sea in the Sea of Azov. In this study we focus on physical mechanisms that govern water exchange through the Kerch Strait, analyse dependence of its direction and intensity on external forcing conditions. Based on ocean color satellite imagery and wind reanalysis data, we show that water transport from the Sea of Azov to the Black Sea is induced by moderate and strong northeastern winds, while water transport in the opposite direction occurs during wind relaxation periods. Thus, direction and intensity of water exchange through the Kerch

15   Strait has wind-govern synoptic and seasonal variability, and do not show dependence on river discharge rate to the Sea of Azov on intra-annual time scale. Finally, we determined numerical dependencies between discharge rate from the Sea of Azov to the Black Sea and spatial characteristics of the related surface-advected plume in the Black Sea, on the one hand, and wind forcing conditions, on the other hand.

1 Introduction

20   The Sea of Azov is an enclosed sea located in the Eastern Europe and is among the smallest and the shallowest seas in the world (Figure 1). Watershed area of the Sea of Azov (586000 km^2) is 15 times greater than the sea area (39000 km^2), therefore, it receives anomalously large river discharge, which annual volume varies in the range of 20 - 54 km^3, that is only of one order less than the sea volume (290 km^3) (Ross, 1977; Ilyin, 2009). 95% of the annual continental discharge is provided by the Don and Kuban rivers that inflow to the northeastern and southeastern parts of the Sea of Azov, respectively

25   (Ross, 1977; Ilyin, 2009). The southern part of the Sea of Azov is connected to the northeastern part of the Black Sea through the long (45 km) and narrow (4-15 km) Kerch Strait. Hydrological characteristics and the general circulation of the Sea of Azov are governed by river runoff and water exchange with the Black Sea. Low water salinity (1-12) (Ross, 1977; Goptarev et al., 1991; Ilyin, 2009) caused by large freshwater discharge and limited water exchange with more saline Black Sea (17-18) (Ivanov & Belokopytov, 2011) through the narrow Kerch Strait is one of the main features of the Sea of Azov.

Thus, the Sea of Azov is a small, shallow, and freshened water body that can be regarded as a large estuary of the Don and Kuban rivers connected with the Black Sea through the Kerch Strait.

Limited water exchange through a narrow strait hinders mixing between connected water bodies which can result in significant differences between their physical and chemical characteristics, as well as between their concentrations of

5   dissolved and suspended constituents. Thus, transport of water masses through a strait and their subsequent spreading in adjacent sea areas can significantly influence many local processes including coastal circulation, primary productivity, water quality, anthropogenic pollution, and deposition of terrigenous material. Impact of water exchange on these processes depend on, first, physical and chemical characteristics of interacting water masses, and, second, variability of water exchange direction, i.e., frequency, duration, and intensity of water exchange periods.

10   Many previous studies were focused on physical, biological, and geochemical processes related to water exchange between two large water bodies through a narrow strait in different World regions, in particular, the Baltic and North Seas through the Danish straits (Matthäus and Lass, 1995; Sayin and Kraus, 1996; Jacobsen and Trebuchet, 2000; Sellschoppa, 2006; She et al., 2007), the Black and Mediterranean seas through the Bosphorus and Dardanelles straits (Yuce, 1996; Andersen et al., 1997; Gregg et al., 1999; Falina et al., 2017; Sozer and Ozsoy, 2017; Stanev et al., 2017), the Mediterranean Sea and the

15   Atlantic Ocean through the Strait of Gibraltar (Garret, 1996; Sannino et al., 2002; Beranger et al., 2005, Soto-Navarro et al., 2015), the Bering and Chukchi seas through the Bering Strait (Woodgate et al., 2010, 2012; Danielson et al., 2014), the Patos Lagoon and the Atlantic Ocean (Castelao and Moller, 2006; Marques et al., 2009). A number of papers addressed structure and variability of circulation in the Kerch Strait (Simonov & Altman, 1991; Lomakin et al., 2010, 2016, 2017; Sapozhnikov, 2011; Chepyzhenko, 2015) and influence of water inflow from the Sea of Azov on coastal ecosystem in the northeastern

20   part of the Black Sea (Lomakin, 2010; Kolyuchkina et al., 2012; Aleskerova et al., 2017; Izhitsky & Zavialov, 2017; Zavialov et al., 2018). However, many aspects of physical background of water exchange through the Kerch Strait and its dependence on external forcing conditions remain unstudied. Also little attention has been paid to spatial characteristics and temporal variability of sub-mesoscale and mesoscale structures formed in the Black Sea and the Sea of Azov as a result of water exchange between these seas.

25   In this study, we address physical mechanisms that drive water exchange between the Sea of Azov to the Black Sea, basing on ocean color satellite imagery, in situ and climatic reanalysis wind data, and river gauge measurements. We reveal dependence of direction and intensity of water exchange through the Kerch Strait on external forcing conditions and analyse temporal variability of these processes from synoptic to intra-annual scales. Also we study dynamics of surface-advected plume of freshened waters from the Sea of Azov spreading in the Black Sea, hereafter, referred as AP, and bottom-advected

30   plume of saline waters from the Black Sea spreading in the Sea of Azov, hereafter, referred as BP. We identify their spatial characteristics, their dependence on external forcing conditions, and analyse their synoptic variability.

The paper is organized as follows. Section 2 provides detailed information about the study region. Satellite, wind, and river discharge data used in this study are described in Section 3. Section 4 focuses on dynamics of inflow and spreading of AP in the Black Sea and BP in the Sea of Azov and dependence of these processes on external forcing conditions on synoptic time

Ocean Science

Discussions

Open Access

EGU

scale. The analysis of frequency, duration, and intensity of water exchange through the Kerch Strait on seasonal, annual, and inter-annual time scales is given in section 5, followed by the conclusions in section 6.

2 Study Area

The Sea of Azov is small and shallow, its average and maximal sea depths are 7 and 14.4 m, respectively. The 10 m isobath
5   is located at a distance of 20-30 km from the sea shore at the eastern, western, and northern parts of the sea, while the southern coastal area is characterized by a narrow (2-5 km) steep slope to a depth of 10 m (Figure 1). The central part of the Sea of Azov is 10-13 m deep and accounts for less than 50% of the sea area. The southern part of the Sea of Azov is connected with the northeastern part of the Black Sea by the Kerch Strait. The narrowest passages of the Kerch Strait are located at its northern (4-5 km) and central (3 km) parts, while at its southern part its width increases up to 15 km. The
10   central part of the Kerch Strait is very shallow (3-5 m) and steadily deepens to depths of 10 and 20 m at its northern and southern parts, respectively. Bathymetry of the northeastern part of the Black Sea is characterized by the narrow shelf, the distance from the shore to the 100 m isobath varies between 15 and 30 km. Further offshore, the steep continental slope descends to a depth of 1000 m at a distance of 50–80 km from the shore (Figure 1).

Large freshwater discharge significantly influences characteristics of the Sea of Azov. The Don River is the largest river
15   inflowing to the Sea of Azov providing approximately 65% of total freshwater runoff to the sea. The Kuban River, which is the second largest river of the study region, provides another 30% of total freshwater runoff. Volumes of annual discharge of the Don and Kuban rivers vary from 18 to 28 km^3 and from 6 to 13 km^3, respectively, which is caused by strong climate and anthropogenic influence (Goptarev et al., 1991; Ilyin et al., 2009). Hydrological characteristics of the Don and Kuban rivers are significantly affected by dams and reservoirs constructed at these rivers. Flow regimes of the Don and Kuban rivers are
20   characterized by long spring-summer freshet during March – June and April – July, respectively, however, discharges during these periods are only twice larger that during the rest of the year (Goptarev et al., 1991; Ilyin et al., 2009). Difference between evaporation and precipitation over the Sea of Azov (17 km^3) is half less than mean annual river runoff (35 km^3) and shows very low inter-annual variability (Ilyin et al., 2009).

Surface temperature of the Sea of Azov is prone to significant seasonal variability from 0 °C in winter to 25 °C in summer
25   caused by shallowness and small volume of the sea (Goptarev et al., 1991; Ilyin et al., 2009). Sea ice covers the northern part of the Sea of Azov every year from December – January to March – April, while its central and southern parts are frozen only during extremely cold winters, which occurred only twice during the last 40 years (Ilyin et al., 2009). Surface salinity in the Sea of Azov varies from 9 to 13 except its more freshened northeastern part, namely, the Taganrog Bay, which receives discharge of the Don River. Large freshwater discharge cause significant horizontal thermohaline gradients in the Sea of
30   Azov. On the other hand, wind-induced mixing penetrates to sea bottom due to shallowness of the Sea of Azov which results in low gradients in vertical thermohaline structure of the sea (Goptarev et al., 1991; Ilyin et al., 2009). Temperature in the surface layer in the northeastern part of the Black Sea also varies in a wide range of values from 7 °C in winter to 23 °C in

summer, while its salinity is 17-19 during the whole year (Ivanov & Belokopytov, 2011). Large freshwater discharge and intense wind-induced vertical circulation result in high concentration of terrigenous sediments, nutrients, chlorophyll a in the Sea of Azov, which is of one order greater than in the northeastern part of the Black Sea (Ilyin et al., 2009).

Circulation in the shallow Sea of Azov is governed mainly by winds, while barolinic forcing is weak (Cherkesov &
5   Shul'ga, 2018). As a result, sea current field shows significant variability in response to different wind forcing conditions. Circulation in the surface layer in the northeastern part of the Black Sea is dominated by a westward current along the continental slope (0.2–0.5 m s^{-1}), which is a part of the Black Sea Rim Current, and an anticyclonic eddy, which is regularly formed between this current and the coast near the Kerch Strait (0.05–0.4 m s^{-1}) (Oguz et al., 1993; Ginzburg et al., 2002; Zatsepin et al., 2003; Korotaev et al., 2003). Level of the Sea of Azov is prone to significant intra-annual and seasonal
10   variability, which is mainly governed by variability of annual river discharge volume, and has order of tens of centimeters, while intra-annual and seasonal variability of the Black Sea level is several centimeters. Synoptic variability of sea level at the coastal areas of the Sea of Azov and the Black Sea, in particular, at the ends of the Kerch Strait is defined by wind surges (Ivanov, 2011; Fomin, 2015; 2017). Tidal amplitudes at the northeastern part of the Black Sea and the Sea of Azov are 2-4 cm; thus, tidal circulation is very low at the study area (Medvedev et al., 2016; Medvedev, 2018).

15   Water transport through the Kerch Strait is an important part of the water budget of the Sea of Azov, however, its characteristics are susceptible to significant uncertainty. Volumes of annual water inflow from the Sea of Azov to the Black Sea and from the Black Sea to the Sea of Azov are estimated as 35-64 and 26-44 km^3, respectively, which is similar to total continental discharge to the Sea of Azov. Current velocity in the Kerch Strait generally exceeds 10 cm s^{-1}, in its narrowest part mean current velocities are 20-30 cm s^{-1}. Barotropic tidal current in the Kerch Strait is less than 5 cm s^{-1} except the
20   narrowest part of the strait where they are equal to 6-10 cm s^{-1} during peak flow (Ferrain et al., 2018). However, 2-days averaged tidal currents in the Kerch Strait are less than 5 cm s^{-1}, therefore, the role of tides in water exchange between the Black and Azov seas can be regarded as negligible. Direction and intensity of water exchange through the Kerch Strait is characterized by significant synoptic variability (Goptarev et al., 1991; Ilyin et al., 2009).

Large salinity difference between the Azov and Black seas results in significantly different spreading and mixing dynamics
25   of waters from the Sea of Azov in the Black Sea and waters from the Black Sea in the Sea of Azov. Inflow of freshened waters from the Sea of Azov to the Black Sea forms a surface-advected AP, which is spreading over wide areas (up to 2000 km^3) in the northeastern part of the Black Sea (Aleskerova et al., 2017). Due to elevated concentrations of terrigenous sediments, nutrients, and anthropogenic pollutants in the waters of the Sea of Azov, AP strongly influences physical, biological, and geochemical processes in the areas adjacent to the Kerch Strait in the northeastern part of the Black Sea
30   (Lomakin, 2010; Kolyuchkina et al., 2012; Aleskerova et al., 2017; Izhitsky and Zavialov, 2017; Zavialov et al., 2018). Processes of inflow, spreading, and mixing of Black Sea water in the Sea of Azov, as well as its influence on local ecosystem received much less attention. Saline waters from the Black Sea form a bottom-advected BP, which can affect large areas in the Sea of Azov, however, its characteristics, spatial structure, and temporal variability remain mainly unstudied.

3 Data and methods

3.1 Data used

Satellite data used in this study include EnviSat MERIS satellite imagery with a spatial resolution of 300 m provided by the European Space Agency (ESA) and Terra MODIS and Aqua MODIS with a spatial resolution of 250 m provided by the

5 National Aeronautics and Space Administration (NASA). MERIS L1 satellite products were downloaded from the ESA web repository (http://merisfrs-merci-ds.eo.esa.int/merci) and used for retrieving maps of sea surface distributions of TSM and Chl-a using the MERIS Case-2 Regional water processing module (Doerffer and Schiller, 2008). MODIS L1 satellite products were downloaded from the NASA web repository (https://ladsweb.modaps.eosdis.nasa.gov/) and used for retrieving maps of sea surface distributions of TSM and Chl-a using the MSL12 processing module. We analyzed 152 MERIS and 110

10 MODIS satellite images of the study region taken in 2002–2012 and 2012–2017, respectively.

The Don and Kuban discharge and local wind forcing data were used to study influence of external forcing conditions on water exchange through the Kerch Strait and spreading of AP in the northeastern part of the Black Sea. The Don and Kuban daily discharge data was obtained from the Razdorskaya and Temryuk gauge stations, respectively, while local wind measurements were performed at the Kerch meteorological station (Figure 1). The atmospheric influence was also examined

15 using wind data obtained from a 6 h NCEP/NCAR reanalysis with a 2.5-degree resolution which showed good accordance with in situ data for the study region (Garmashov et al., 2016). We used zonal and meridional wind components from the only reanalysis grid point located at the study area (44.7611° N, 35.625° E) which were validated against in situ wind measurements.

3.2 Identification of AP and BP by satellite imagery

20 As it was discussed in Section 3.1, waters of the Azov and Black seas have very different physical and chemical properties. As a result, different ocean surface characteristics measured by satellite instruments can be used to study spreading of surface-advected AP in the northeastern part of the Black Sea. Previous related studies used sea surface temperature (SST) and concentrations of chlorophyll a (Chl-a) and total suspended matter (TSM) retrieved from optical satellite data (Ivanov & Belokopytov, 2011; Aleskerova et al., 2017). However, all these characteristics are prone to significant variability and/or do

25 not act as passive tracers, which hinders their direct application for accurate identification of borders of AP.

First, difference in SST between the southern part of the Sea of Azov and the northeastern part of the Black Sea varies from -4 °C in winter to 4 °C in summer (Aleskerova et al., 2017). On the other hand, diurnal variability of SST in the coastal areas of the Sea of Azov and the Black Sea is also equal to several degrees (Ivanov & Belokopytov, 2011; Chepyzhenko, 2015). This fact prevents formation of distinctive frontal zones between AP and the adjacent sea, especially if AP is formed by

30 inflow from the Sea of Azov during several days, i.e. several diurnal temperature cycles of SST. As a result, SST satellite products can be limitedly used for effective detection of borders of AP. TSM provides a clear optical signal of turbid AP in the Black Sea due to large difference in suspended sediment concentration between the Azov and Black seas (Lomakin,

2017). However, wind-induced resuspension of sea bottom sediments, which regularly occurs along the shallow northeastern coast of the Black Sea, cause increase of TSM, which can exceed mean TSM values of AP. As a result, usage of TSM for identifying spreading area of AP can be misleading that is illustrated by Fig. 2. Thus, we used Chl-a as a stable tracer of AP in the Black Sea, that is consistent with a number of previous studies focused on tracking of buoyant plumes with satellite
5   ocean color data (e.g., Dzwonkowski et al., 2007; Piola et al., 2008).

4 Results

4.1 Spreading of AP in the Black Sea

River discharge to the Sea of Azov and wind forcing at the area of the Kerch Strait are the main factors that are believed to govern inflow of freshened waters from the Sea of Azov to the Black Sea, hereafter referred as AI (Goptarev et al., 1991;
10   Simonov & Altman, 1991; Ivanov & Belokopytov, 2011). We analyzed MERIS and MODIS optical satellite imagery acquired during 2002-2017 and identified 48 AI events. Basing on wind reanalysis data and gauge data of the Don and Kuban rivers we studied dependence of formation of AI events on river discharge and wind forcing conditions on synoptic and seasonal time scales.

First, we analyzed relation between concentration of Chl-a in the Kerch Strait and the adjacent area of the Black Sea
15   retrieved from optical satellite imagery, on the one hand, and direction of wind forcing averaged over 24 hours preceding satellite observations, on the other hand (Figure 3). Elevated concentrations of Chl-a, which is regarded as the main indicator of an AI event, were observed only if azimuthal angle of wind direction was between 210 and 260º and wind velocity exceeded 5 m/s. It can be seen that the resulting wind direction range corresponds to the northeastern wind and formation of an AI event is induced only by moderate and strong northeastern winds. Second, we addressed relation between
20   concentration of Chl-a and discharge rates of the Don and Kuban Rivers (Figure 4). We obtained that AI events are formed under the whole variety of discharge conditions and do not show any dependence on discharge rate on synoptic time scale. Synoptic variability of river discharge strongly influences water exchange between a river estuary and open sea if volume of an estuary is relatively small as compared to river discharge rate (Officer, 1976; Sheldon & Alber, 2002; Wang et al., 2004). However, volume of the Sea of Azov, regarded as an estuary of the Don and Kuban rivers, is of one order greater than
25   annual freshwater runoff. As a result, signal of synoptic variability of river discharge dissipates in the Sea of Azov and does not influence formation of AI events. Thus, we obtain that AI events are induced by wind forcing and do not depend on river discharge conditions on synoptic time scale.

AI event, i.e., inflow of freshened waters from the Sea of Azov to the Black Sea, causes formation of buoyant AP. Spreading of a buoyant plume in a non-tidal sea is mainly governed by discharge rate and wind forcing (Fong et al., 1997; Hallock &
30   Marmorino, 2002; Horner-Devine et al., 2015) and is characterized by strong variability of size, shape, and spreading patterns under different configurations of external forcing conditions (Kourafalou et al., 1996; Xia et al., 2007; Zavialov et al., 2014; Osadchiev, 2015; Osadchiev et al., 2016).

However, analysis of satellite imagery revealed stability of spreading pattern of AP. All satellite images where AI event was detected showed that AP propagated westward along the southeastern shore of the Crimean Peninsula (Figure 2b). This freshened alongshore current formed by AP dissipated on a distance of 50-200 km from its source at the Kerch Strait. AP did not spread eastward along the coast of the Taman Peninsula or southward to the open sea at any of the analyzed satellite images. In particular, elevated values of TSM to the east from the Kerch Strait along the Taman Peninsula, which are regularly observed at satellite imagery, are not accompanied by elevated values of Chl-a (Figure 2a). This fact indicates that these turbidity features at sea surface layer are induced by bottom resuspension and do not correspond to eastward spreading of AP along the coast of the Taman Peninsula.

Stability of spreading pattern of AP can be explained in the following way. As it was shown above, AI occurs only during northeastern wind and causes formation of AP. Thus, initial spreading of AP from its source at the Kerch Strait is forced by northeastern wind. As a result, the AP forms a quasi-geostrophic coastal current in response to downwelling favorable wind forcing, which was addressed in many previous studies (Garvine, 1987; Yankovsky & Chapman, 1997; Fong and Geyer, 2002). Spreading of AP in different direction, e.g., southward or eastward, requires change of direction of wind forcing. However, change of wind direction will also result in cessation of inflow of freshened water to the Black Sea and cause dissipation of the freshened alongshore current.

Spatial scales of AP identified at satellite imagery shows significant synoptic variability. In particular, during an individual AI event alongshore extent and area of AP can increase from 60 to 150 km and from 400 to 1300 km^2, respectively, during several days (Figure 5). On the other hand, AP dissipates during several days after the end of AI event. As it was shown above, intensity of AI, i.e., freshwater discharge rate, depends on local wind, which is, therefore, the only critical external force that governs synoptic variability of spatial scales of AP. Thus, we can reconstruct dependence of spatial characteristics of AP identified at satellite imagery on speed and duration of northeastern wind forcing. For this purpose, we used a wind forcing index $W_t = v_t \cdot t$, [h*km/h] where v_t is average wind velocity during the time period t when wind direction was between 210 and 260º.

Alongshore extent and area of AP were identified at 48 satellite images obtained during or shortly after northeastern wind forcing conditions. For every registered AP we calculated values of its alongshore extent (L), area (S), and wind forcing index W_t for a period of predominant northeastern wind forcing preceding time of satellite observations. For all these cases W_t exceeded 500 km, therefore, we presume this value as a threshold for formation of an AI event. Figures 6 illustrate the obtained linear relations between logarithms L and S, on the one hand, and logarithm of W_t, on the other hand: $\lg(L) = 0.4 + 0.53 \cdot \lg(W_t)$; $\lg(S) = 0.53 + 0.77 \cdot \lg(W_t)$. The obtained equations reveal that dependences between spatial characteristics of AP and wind forcing index follow a power law: $L = 2.5 \cdot W_t^{0.53}$ (RMSE is about 9 km); $S = 3.4 \cdot W_t^{0.77}$ (RMSE is about 136 km^2).

Finally, we analyzed dependence of seasonal variability of area of AP, which is indicative of intensity of AI, on wind forcing and river discharge conditions. For this purpose we calculated monthly averages of area of AP detected at optical satellite imagery and compared them with monthly averages of wind forcing index and total discharge rate of the Don and Kuban rivers (Figure 7). Monthly variability of average area of AP shows direct relation with monthly variability of wind forcing

index. The obtained graph reveals that both characteristics have similar monthly variations with two distinct peaks in September and December – March and lowest values in May – June.

However, the opposite situation is observed for dependence between monthly averages of area of AP and river discharge rate. Several studies showed that variability of the Don and Kuban discharges induces variability of level of the Sea of Azov,

5   thus, presumably influencing formation of AI events on seasonal time scale (Goptarev et al., 1991; Filippov, 2015). Nevertheless, seasonal variability of river discharge characterized by distinct spring freshet and autumn-winter draught showed no relation with intensity of AI events. Thus, we obtain that river discharge does not govern seasonal variability of AI.

4.2 Spreading of BP in the Sea of Azov

10   Inflow of saline waters from the Black Sea to the Sea of Azov, hereafter referred as BI, causes formation of a BP. Density of BP is significantly larger than density of surrounding waters of the Sea of Azov. As a result, it is spreading in the bottom layer and cannot be directly identified at satellite imagery. However, wind-induced mixing, which can penetrate to sea bottom at the shallow Sea of Azov, can cause mixing of low-turbid water of BP with overlaying water of the Sea of Azov, thus, decreasing surface turbidity above the spreading area of BP. As a result, presence of BP in the bottom layer can be

15   identified at satellite imagery as low-turbidity area in the Sea of Azov adjacent to the Kerch Strait (Figure 8). If these low-turbid areas associated with spreading of BP are large enough, they occupy the deepest part of the Sea of Azov and their contours correspond to bathymetric isolines (Figure 9). This fact is presumably caused by spreading dynamics of dense BP, which tends to flow down the slope of the Sea of Azov due to gravity force and accumulate in the central basin of the Sea of Azov.

20   We analyzed MERIS and MODIS optical satellite imagery acquired during 2002-2017 and identified 12 BI events. The process of formation of BI events does not show dependence on southwestern wind forcing, as was revealed for AI events and northeastward winds. On the opposite, BI events were detected during all types of wind forcing except during and shortly after moderate and strong northeastern winds. Figures 8-9 illustrate typical cases of formation of BI event in response to local wind forcing. Strong northeastern wind (up to 15 m/s) observed during 14-21 April 2003 caused formation of AP,

25   which was followed by light and variable wind on 21-27 April 2003 and formation of BP detected at satellite imagery on 27 April 2003 (Figure 8). A large BP occupying approximately 10000 km^2 in the deep central basin of the Sea of Azov was observed on 23 June 2007. The observation time was preceded by 14 days of light and variable wind (10-23 July 2007), while on 5-10 June 2007 northeastern wind caused formation of AP observed on 6 July 2007 (Figure 9).

As it was shown above, northeastern wind causes formation of AI event and prevents formation of BI event. BI event, in its

30   turn, is formed in absence of northeastern wind and area of BP depends on duration of this period. This feature can be explained in the following way. Saline and dense water of the Black Sea tends to form a bottom-advected gravity flow to the Sea of Azov through the Kerch Strait. In presence of northeastern wind forcing, wind stress is transferred into a relatively shallow Sea of Azov and induces intense flow of freshened water from the area adjacent to the Kerch Strait to the Black Sea.

The Kerch Strait is very shallow, especially at its central part, which is 3-5 m deep. Thus, this wind-induced surface flow occupies the whole water column in the Kerch Strait and prevents formation of gravity-induced flow in the opposite direction in bottom layer. After the end of a period of northeastern wind forcing and cessation of AI, gravity flow from the Black Sea to the Sea of Azov is restored and BP is formed. As a result, area of BP depends on duration of the period without
5 northeastern wind forcing.

Similar configuration of water exchange between the large Patos Lagoon and the Atlantic Ocean through the narrow strait was described by Castelao and Moller (2006). They revealed formation of a reverse flow of saline ocean water to the lagoon after an outflow of freshened lagoon water induced by wind forcing. This feature is caused by reverse of pressure gradient in the lagoon after end of an outflow-favorable wind forcing event. . Our results are also supported by direct measurements of
10 vertical current profiles performed by ADCP instruments in the southern and northern parts of the Kerch Strait during 26-28 September 2011 and reported by Ivanov (2012). These measurements showed that moderate northeastern winds observed on 26-27 September induced surface-to-bottom northward flow in the shallow northern part of the Kerch Strait. However, both wind-induced southward surface flow and gravity-induced northward bottom flow were detected in the deep southern part of the strait. Light western wind observed on 28 September 2011 resulted in termination of southward surface flow in both parts
15 of the strait and formation of a distinct gravity-induced northward flow.

5 Discussion

Analysis of satellite imagery and wind data described in Section 4.1 showed that northeastward wind forcing governs formation of AI events and spreading of AP on synoptic and seasonal time scales. Thus, we can reconstruct dependence of intensity of AI, i.e., discharge rate from the Sea of Azov to the Black Sea through the Kerch Strait, on speed and duration of
20 local wind forcing. First, we define "AI-favorable" wind conditions as a period of predominant northeastern wind forcing, which wind forcing index T_v exceeds 500 km. All other periods are prescribed as "BI-favorable" wind conditions. Second, wind reanalysis for the study region, we identify periods of AI-favorable wind events. Finally, we calculate areas of AP formed during these events using the obtained relation between wind forcing index and area of AP. Sum these areas for all AI events occurred during a year (S_{AP}) is indicative of total annual volume of water inflow from the Sea of Azov to the Black
25 Sea through the Kerch Strait (V_{AI}). Simonov & Altman (1991) estimate mean value of V_{AI} during 1963-1972 as 64.3 km^3, while we calculated that mean value of S_{AP} during 1963-1972 is equal to 12747 km^2. We assume that mean depth of AP (H_{AP}) does not significantly depend on its spatial scale and is mainly defined by bathymetry of the Kerch Strait. Thus, we obtain that $V_{AI} = H_{AP} S_{AP}$ and mean annual depth of AP is $H_{AP} = V_{AI} / S_{AP} = 5$ m, which is consistent with depth of the Kerch Strait (Figure 1). Finally, using the dependence of plume area on wind forcing index and estimation of mean depth of AP we
30 obtain the following equation for water inflow volume during an AI event (V): $V = S \cdot H_{AP} = 0.017 \cdot W_t^{0.77}$.

Basing on the equations described above, we estimated mean monthly and annual frequency, duration, and share of AI-favorable and BI-favorable wind conditions during the period of 2000-2017 and calculated volume of discharge from the Sea

of Azov to the Black Sea (table 1). The most frequent and long AI-favorable wind conditions are registered in autumn and winter. AI events occur during 36-39% of days in these months except a distinct peak in October, when they account for 52% of days. Then their frequency decreases from 2.2-3.1 times a month in September – February to 0.9-1.2 times a month in May – July that results in decrease of share of AI events to 11-15% of days during the latter period. On the other hand,

5   mean monthly duration of AI-favorable wind conditions is stable during the year and varies from 91.4 hour in June to 119.1 in October. BI-favorable wind conditions, on the opposite, are dominating in May – July (85-89% of days) and then their share steadily decreases till October (48% of days). Frequency of BI events is the same as frequency of AI events, while mean monthly duration of BI events shows significantly greater seasonal variability from 135 hours in October to 718.5 in June. Monthly volumes of discharge from the Sea of Azov to the Black Sea is also stable and varies from 3.54 km^3 in June to

10   5.68 km^3 in January. Mean annual discharge volume during 2000-2017 is estimated equal to 53.69 km^3 that shows good accordance with previous estimations of this value as 55 km^3 (Goptarev, 1991).

6 Conclusions

In this work we studied water exchange between the Sea of Azov to the Black Sea through the Kerch Strait. We revealed that different physical mechanisms govern water transport in southward (from the Sea of Azov to the Black Sea) and northward

15   (from the Black Sea to the Sea of Azov) directions. Southward AI events are induced by moderate and strong northeastern wind forcing. In this case, wind stress causes transport of freshened water from shallow southern part of the Sea of Azov through the Kerch Strait that results in formation of a buoyant plume in the Black Sea. This surface-advected AP is characterized by elevated concentrations of suspended sediments and chlorophyll a and is distinctly visible at optical satellite imagery. AP is spreading off the Kerch Strait as a quasi-geostrophic coastal current along the southeastern shore of the

20   Crimean Peninsula, its area steadily increases during an AI event that last 1-5 days. As a result, AP occupies large area in the northeastern part of the Black Sea up to 2000 km^2. However, AP dissipates during 1-5 days after end of AI event. The short-term, but regular process of formation and spreading of AP at the northeastern part of the Black Sea influences many local physical, biochemical, and geological processes, which were addressed in many previous studies.

Northward water transport in the Kerch Strait, on the opposite, was registered after relaxation of strong northeastward winds.

25   Saline and dense water from the Black Sea propagates through the Kerch Strait and inflows to the freshened Sea of Azov as a bottom-advected flow that is induced by the gravity force. Strong northeastern wind plays a restricting role for this process, because intense wind-induced southward surface flow of water from the Sea of Azov occupies the whole water column in the shallow central part of the Kerch Strait. This prevents formation of the gravity-induced flow of water from the Black Sea in the opposite direction in the bottom layer. Analysis of satellite images did not show any direct dependence of northward

30   water transport in the Kerch Strait on characteristics of local wind forcing. However, this feature can be caused by relatively low number of detected BI events at satellite imagery, therefore future study of influence of wind forcing on this process require more specific and detailed in situ measurements and/or numerical modelling in the study region.

After water from the Black Sea inflows to the Sea of Azov it forms a bottom-advected BP that tends to spread down the slope due to gravity force and accumulate in the deep central basin of the Sea of Azov. Area of BP depends on duration of the related BI event, i.e., period without northeastern wind forcing that can last up to 13 days. BP exhibits intense mixing with overlaying freshened waters caused by frequent wind-induced turbulence that penetrates to sea bottom in the shallow
5 Sea of Azov. This results in formation of area of low turbid water in the surface layer that is visible at optical satellite imagery and indicates location of BP in the Sea of Azov.

We determined that wind forcing governs direction and intensity of water transport in the Kerch Strait on inter-annual time scale. River runoff to the Sea of Azov does not show any distinct influence on synoptic and seasonal variability of water exchange through the Kerch Strait which is not typical for river estuaries, including large ones, e.g., the Patos Lagoon
10 (Castelao and Moller, 2006) and the Amur Liman (Osadchiev, 2017). We presume that this feature is caused by large volume of the Sea of Azov (290 km^3), which is of one order larger than annual continental discharge to the sea ($20 – 54$ km^3).As a result, river runoff during flooding period increases level of the Sea of Azov only by 6-7 centimeters as compared to draught period. Volume of the Patos Lagoon (50 km^3), on the opposite, is of the same order as continental runoff volume (75 km^3), which causes increase of lagoon level by 70-80 cm during freshet periods. As a result, stable seaward flow from the Patos
15 Lagoon during the seasonal flood can be reversed only by very strong winds (Moller and Castaing, 1999). Volume of the Amur Liman (20 km^3) is much less than the annual Amur discharge volume (400 km^3), therefore, water exchange between the Amur Liman and sea is dominated by river regime during the major part of a year (Osadchiev, 2017). On the other hand, several previous studies reported that inter-annual river discharge variability influence water exchange between the Sea of Azov and the Black Sea (Goptarev, 1991; Ilyin et al., 2009; Ivanov & Belokopytov, 2011). However, detailed analysis of
20 inter-annual variability of water transport in the Kerch Strait and its dependence on external factors is beyond the current article.

In this study we revealed wind forcing conditions that cause formation of AI and BI events and analyzed intra-annual variability of their monthly and annual frequency and duration for the period of 2000-2017. BI-favorable wind conditions are significantly more frequent than AI-favorable conditions and occur during 71% of days in a year with a distinct peak in May
25 – July (85-89% of days). AI events slightly dominate over BI events only in October (58% of days), while during the rest of the year their share is 11-39%. Shifts between AI-favorable and BI-favorable wind conditions occur relatively rarely, 1-3 times in a month and only 46 times in a year. Thus, AI and BI events generally last for relatively long time periods; their mean annual durations are approximately 4.3 and 13.7 days, respectively. Duration of AI events does not significantly change during a year, while mean monthly duration of BI event varies from 5 to 30 days.

30 Basing on satellite and wind reanalysis data we derived numerical equation that define discharge rate from the Sea of Azov to the Black Sea during AI event on speed and duration of northeastern wind. Using this equation, we calculated monthly averages of water transport from the Sea of Azov to the Black Sea during 2000-2017 which showed low seasonal variability. Also we obtained relations between spatial characteristics of AP, namely, alongshore scale and area, on wind forcing conditions during AI event. On the other hand, we did not determine relevant equations for water transport from the Black

Sea to the Sea of Azov. It is caused by the fact that spatial characteristics and temporal variability of spreading of BP in the bottom layer of the Sea of Azov is much worse detected at satellite imagery, as compared to surface-advected AP. As a result, definition of dependencies for both discharge rate from the Black Sea to the Sea of Azov and spatial characteristics of BP on wind forcing requires specific in situ measurements which are beyond the current study.

5 A big number of previous studies were focused on numerical modelling of circulation, food webs, water quality, transport and fate of dissolved and suspended matter and other processes in the Black Sea (e.g., Stanev, 1990; Oguz et al., 1995; Stanev & Staneva, 2000; Staneva et al., 2001; Enriquez et al., 2005; Korotenko et al., 2010; Korotenko, 2017, Stanev et al., 2017). Many of these studies did not simulate circulation in the Sea of Azov and the Kerch Strait, but reproduced water exchange through the Kerch Strait as a border condition. However, these works generally applied mean annual or mean

10 seasonal exchange values and neglected the fact that direction and discharge rates of water transport through the Kerch Strait have strongly inhomogeneous temporal distributions and significant inter-annual variability. In particular, we are not aware of any relevant numerical parameterizations of water exchange through the Kerch Strait that reproduce its synoptic variability. Thus, the equations, which define conditions of formation of AI events and dependence of discharge rate during AI event on speed and duration of northeastern wind, that were obtained in the current study, hold promise to be useful for

15 numerical modelling of the Black Sea. They can improve existing parameterizations of border conditions at the Kerch Strait and, therefore, increase accuracy of numerical simulation of many physical, geological, and biochemical processes in the Black Sea.

Data availability

The Envisat MERIS satellite data were downloaded from the European Space Agency repository of the Envisat satellite data

20 http://merisfrs-merci-ds.eo.esa.int/merci (available after registration). The Terra MODIS and Aqua MODIS satellite data were downloaded from the National Aeronautics and Space Administration repository of LANCE-MODIS satellite data https://lance3.modaps.eosdis.nasa.gov. The river discharge and wind data were downloaded from the Federal Service for Hydrometeorology and Environmental Monitoring of Russia repositories http://gis.vodinfo.ru (available after registration) and https://rp5.ru. The NCEP/NCAR reanalysis data were downloaded from the National Oceanic and Atmospheric

25 Administration website https://www.esrl.noaa.gov/psd/data/gridded/data.ncep.reanalysis.surface.html.

Competing interests

The authors declare that they have no conflict of interest.

Ocean Science
Discussions

Open Access

EGU

References

Aleskerova, A. A., Kubryakov, A. A., Goryachkin, Y. N., & Stanichny, S. V.: Propagation of waters from the Kerch Strait in the Black Sea, Physical Oceanography, 6, 47–57, doi:10.22449/1573-160X-2017-6-47-57, 2017

Andersen, S., Jakobsen, Fl., Alpar, B.: The water level in the Bosphorus Strait and its dependence on atmospheric forcing,
10   German Journal of Hydrography, 49, 466-475, doi:10.1007/BF02764341, 1997

Beranger, K., Mortier, L., Crepon, M.: Seasonal variability of water transport through the Straits of Gibraltar, Sicily and Corsica, derived from a high-resolution model of the Mediterranean circulation. Progress in Oceanography, 66, 341-364, doi:10.1016/j.pocean.2004.07.013, 2005

Castelao R.M. & Moller Jr. O.O.: A modeling study of Patos lagoon (Brazil) flow response to idealized wind and river
15   discharge: dynamical analysis, Brazilian journal of oceanography, 54(1), 1-17, doi:10.1590/S1679-87592006000100001, 2006

Chepyzhenko, A.A., Chepyzhenko, A.I., & Kushnir, V.M.: Strait of Kerch water structure derived from the data of contact measurements and satellite imagery, Oceanology, 55, 47-55, doi:10.1134/S0001437015010038, 2015

Cherkesov, L. V. & Shul'ga, T. Y.: Numerical Analysis of the Effect of Active Wind Speed and Direction on Circulation of
20   Sea of Azov Water with and without Allowance for the Water Exchange through the Kerch Strait, Oceanology, 58, 19-27, doi:10.1134/S0001437018010022, 2018

Danielson, S. L., Weingartner, T. W., Hedstrom, K., Aagaard, K., Woodgate, R.,Curchitser, E., Stabeno, P.: Coupled wind-forced controls of the Bering–Chukchi shelf circulation and the Bering Strait through-flow: Ekman transport,continental shelf waves, and variations of the Pacific-Arctic sea surface height gradient, Progress in Oceanography, 125, 40–61,
25   doi:10.1016/j.pocean.2014.04.006, 2014

Dzwonkowski, B. & Yan, X. H.: Tracking of a Chesapeake Bay estuarine outflow plume with satellite-based ocean color data, Continental Shelf Research, 25, 1942–1958, doi:10.1016/j.csr.2005.06.011, 2007

Enriquez, C. E., Shapiro, G.I., Souza, A.J., Zatsepin, A.G.: Hydrodynamic modelling of mesoscale eddies in the Black Sea, Ocean Dynamics, 55 (5-6), 479–489, doi:10.1007/s10236-005-0031-4, 2005
30   Falina, A., Sarafanov, A., Ozsoy, E., & Turuncoglu, U. U.: Observed basin-wide propagation of Mediterranean water in the Black Sea, Journal of Geophysical Research, 122(4), 3141–3151, doi:10.1002/2017JC012729, 2017

Ferrain, C., Bellafiore, D., Sannino, G., Bajo, M., & Umgiesser, G.: Tidal dynamics in the inter-connected Mediterranean, Marmara, Black and Azov seas, Progress In Oceanography, doi:10.1016/j.pocean.2018.02.006, 2018

Filippov, Y.G.: The impact of the Don River runoff on the water level in the Taganrog Bay, Russian Meteorology and Hydrology, 40, 127, doi:10.3103/S1068373915020090, 2015

5   Fomin, V. V., Lazorenko, D. I., Fomina, I. N.: Numerical modeling of water exchange through the Kerch Strait for various types of the atmospheric impact, Physical Oceanography, 4, 79, doi: 10.22449/1573-160X-2017-4-79-89, 2017

Fomin, V. V., Polozok, A. A., Fomina, I. N.: Simulation of the Azov Sea Water circulation subject to the river discharge, Physical Oceanography, 1, doi: 10.22449/1573-160X-2015-1-15-26, 2015

Fong, D. A., & Geyer, W. R.: The alongshore transport of freshwater in a surface-trapped river plume, Journal of Physical

10   Oceanography, 32, 957–972, doi:10.1175/1520-0485(2002)032<0957:TATOFI>2.0.CO;2, 2002

Fong, D. A., Geyer, W. R., & Signell, R. P.: The wind-forced response on a buoyant coastal current, Observations of the western Gulf of Maine plume, Journal of Marine Systems, 12(1-4), 69-81, doi:10.1016/S0924-7963(96)00089-9, 1997

Garmashov, A. V., Kubryakov, A. A., Shokurov, M. V., Stanichny, S. V., Toloknov, Y. N., & Korovushkin, A. I.: Comparing satellite and meteorological data on wind velocity over the Black Sea. Izvestiya, Atmospheric and Oceanic

15   Physics, 52(3), 309-316, doi:10.1134/S000143381603004X, 2016

Garvine, R. W.: Estuary plumes and fronts in shelf waters: A layer model, Journal of Physical Oceanography, 17, 1877–1896, doi:10.1175/1520-0485(1987)017<1877:EPAFIS>2.0.CO;2, 1987

Ginzburg, A. I. Kostianoy, A.G., Krivosheya, V.G., Nezlin, N.P., Soloviev, D.M., Stanichny, S.V., Yakubenko, V.G., (2002), Mesoscale eddies and related processes in the northeastern Black Sea, Journal of Marine Systems, 32, 71–90,

20   doi:10.1016/S0924-7963(02)00030-1, 2002

Goptarev, N. P., Simonov, A. I., Zatuchnaya, B. M., Gershanovich, D. E.: Hydrometeorology and Hydrochemistry of the Soviet Seas, Vol. 5, The Sea of Azov., St. Petersburg, Gidrometeoizdat (in Russian), 1991

Gregg, M. C., Ozsoy, E, Latif, M. A.: Quasi-steady exchange flow in the Bosphorus, Geophysical Research Letters, 26(1), 83–86, doi.org/10.1029/1998GL900260, 1999

25   Hallock, Z.R., Marmorino, G.O.: Observations of the response of a buoyant estuarine plume to upwelling favourable winds, Journal of Geophysical Research, 107(C7), 3066, doi:10.1029/2000JC000698, 2002

Horner-Devine, A. R., Hetland, R. D., & MacDonald, D. G.: Mixing and transport in coastal river plumes, Annual Review of Fluid Mechanics, 47(47), 569–594, doi:10.1146/annurev-fluid-010313-141408, 2015

Ilyin, Yu. P., Fomin, V. V., D'yakov, N. N., & Gorbach, S. B.: Hydrometeorological Conditions of the Ukraine Seas. Vol. 1.

30   The Azov Sea, Sevastopol, ECOSI-Gidrofizika (in Russian), 2009

Ivanov, V. A., & Belokopytov, V. N.: Oceanography of the Black Sea, Sevastopol, ECOSI-Gidrofizika, 2013

Ivanov, V. A., Cherkesov, L. V., Shul'ga, T. Y.: Extreme deviations of the sea level and the velocities of currents induced by constant winds in the Azov Sea, Physical Oceanography. 21, 98–105, doi:10.1007/s11110-011-9107-5, 2011

Ivanov, V. A., Morozov, A. N., Kushnir, V. M., Shutov, S. A., Zima, V. V.: Currents in the Kerch Strait, adcp-observations, September, 2011. Ecological safety of coastal and shelf zones and complex usage of shelf resources, 26-1, 170-178 (in Russian), 2012

Izhitskiy, A. S., & Zavialov, P. O.: Hydrophysical state of the Gulf of Feodosia in May 2015, Oceanology, 57, 485–491, doi:10.1134/S0001437017040105, 2017

Jakobsen, F., & Trébuchet, C.: Observations of the transport through the Belt Sea and an investigation of the momentum balance, Continental Shelf Research, 20(3), 293-311, doi:10.1016/S0278-4343(99)00073-4, 2000

Kolyuchkina, G.A., Belyaev, V.A., Spiridonov, V.A., Simakova, U.V.: Long-term effects of Kerch Strait residual oil-spill: hydrocarbon concentration in bottom sediments and biomarkers in Mytilus galloprovincialis (Lamarck, 1819), Turkish Journal of Fisheries and Aquatic Sciences, 12, 461-469, doi: 10.4194/1303-2712-v12_2_37, 2012

Korotaev, G., Oguz, T., Nikiforov, A., & Koblinsky, C.: Seasonal, interannual, and mesoscale variability of the Black Sea upper layer circulation derived from altimeter data, Journal of Geophysical Research, 108(C4), 3122, doi:10.1029/2002JC001508, 2003

Korotenko, K. A.: Modeling processes of the protrusion of near-coastal anticyclonic eddies through the Rim Current in the Black Sea, Oceanology, 57, 394-401, doi:10.1134/S0001437017020114, 2017

Korotenko, K. A., Malcolm, J. B, & David, E. D.: High-resolution numerical model for predicting the transport and dispersal of oil spilled in the Black Sea, Terrestrial Atmospheric and Oceanic Sciences, 21, 123-136, doi:10.3319/TAO.2009.04.24.01(IWNOP, 2010

Kourafalou, V. H., Lee, T. N., Oey, L., & Wang, J.: The fate of river discharge on the continental shelf: 2.Transport of coastal low-salinity waters under realistic wind and tidal forcing, Journal of Geophysical Research, 101, 3435–3456, doi:10.1029/95JC03025, 1996

Lomakin, P. D., Chepyzhenko, A. I., Chepyzhenko, A. A.: Field of the colored dissolved organic matter concentration in the Sea of Azov and the Kerch Strait waters based on optical observations, Physical Oceanography, 5, doi: 10.22449/1573-160X-2016-5-71-83, 2016

Lomakin, P. D., Chepyzhenko, A. I., Chepyzhenko, A. A.: The total suspended matter concentration field in the Kerch strait based on optical observations, Physical Oceanography, 6, doi:10.22449/1573-160X-2017-6-58-69, 2017

Lomakin, P. D., Panov, D. B., & Spiridonova, E. O.: Specific features of the inter-annual and seasonal variations of hydrometeorological conditions in the region of Kerch Strait for the last two decades, Physical Oceanography, 20, 109-121. doi:10.1007/s11110-010-9071-5, 2010

Marques, W.C., Fernandes, E.H., Monteiro, I.O., Moller, O.O.: Numerical modeling of the Patos Lagoon coastal plume, Brazil, Continental Shelf Research, 29, 556-571, doi: 10.1016/j.csr.2008.09.022, 2009

Matthäus, W. & Lass H.U.: The Recent Salt Inflow into the Baltic Sea, Journal of Physical Oceanography, 25(2), 280-288, doi:10.1175/15200485(1995)025<0280:TRSIIT>2.0.CO;2, 1995

Medvedev, I. P.: Tides in the Black Sea: observations and numerical modelling, Pure and Applied Geophysics, 175, 1951–1969, doi:10.1007/s00024-018-1878-x, 2018

Medvedev, I. P., Rabinovich, A. B., & Kulikov, E. A.: Tides in three enclosed basins: the Baltic, Black, and Caspian seas. Frontiers in Marine Science, 46 (3), doi:10.3389/fmars.2016.0004, 2016

5   Miranda, L. B., Andutta, F. P., Kjerfve, B., & de Castro Filho, B. M.: Fundamentals of estuarine physical oceanography (Vol. 8). Springer, Singapore, doi:10.1007/978-981-10-3041-3, 2017

Moller, O.O. and Castaing, P.: Hydrographical Characteristics of the Estuarine Area of Patos Lagoon (30° S, Brazil). In: Estuaries of South America. Their Geomorphology and Dynamics, ed. G.M.E. Perillo, M.C. Piccolo, and M.P. Quivira, 83–100, Berlin: Springer-Verlag, 1999

10   Officer, C.B.: Physical Oceanography of Estuaries (and associated coastal waters), Wiley, New York, doi:10.4319/lo.1977.22.5.0975, 1976

Oguz, T., Latun, V. S., Latif, M. A., Vladimirov, V. V., Sur, H. I., Makarov, A. A., et al.: Circulation in the surface and intermediate layers of the Black Sea. Deep Sea Research Part I, Oceanographic Research Papers, 40, 1597–1612, doi:10.1016/0967-0637(93)90018-X, 1993

15   Osadchiev, A. A.: A method for quantifying freshwater discharge rates from satellite observations and Lagrangian numerical modeling of river plumes, Environmental Research Letters, 10, 085009, doi:10.1088/1748-9326/10/8/085009, 2015

Osadchiev, A.A.: Spreading of the Amur river plume in the Amur Liman, the Sakhalin Gulf, and the Strait of Tartary, Oceanology, 57, 376-382, doi: 10.1134/S0001437017020151, 2017

Osadchiev, A. A., Korotenko, K. A., Zavialov, P. O., Chiang, W.-S., & Liu, C.-C.: Transport and bottom accumulation of

20   fine river sediments under typhoon conditions and associated submarine landslides: case study of the Peinan River, Taiwan, Natural Hazards and Earth System Sciences, 16, 41-54, doi:10.5194/nhess-16-41-2016, 2016

Piola, A. R., Romero, S. I., & Zajaczkovski, U.: Space-time variability of the Plata plume inferred from ocean color, Continental Shelf Research, 28, 1556–1567, doi:10.1016/j.csr.2007.02.013, 2008

Ross, D. A.: The Black Sea and the Sea of Azov. In Nairn, A.E.M., Kanes, W.H., Stehli, F.G., et al. The Ocean Basins and

25   Margins (Vol. 4A, pp. 445-481). Springer, Boston, MA, doi:10.1007/978-1-4684-3036-3_11, 1977

Sannino, G., Bargagli, A., & Artale, V.: Numerical modelling of the mean exchange through the Strait of Gibraltar, Journal of Geophysical Research, 107(C9), 1–24, doi:10.1029/2001JC000929, 2002

Sapozhnikov, V. V., Kumantsov, M. I., Agatova, A. I., Arzhanova, N. V., Lapina, N. M., Roi, V. I., et al.: Complex investigations of the Kerch Strait. Oceanology, 51, 896, doi:10.1134/S0001437011050146, 2011

30   Sayin, E., & Krauß, W.: A numerical study of the water exchange through the Danish Straits. Tellus A, 48(2), 324-341, doi:10.1034/j.1600-0870.1996.t01-1-00009.x, 1996

Sellschoppa, J., Arneborgb, L., Knolla, M., Fiekasa, V., Gerdesa, F., Burchardc, H., et al.: Direct observations of a medium-intensity inflow into the Baltic Sea, Continental Shelf Research, 26, 2393–2414, doi: 10.1016/j.csr.2006.07.004, 2006

She, J., Berg, P., & Berg, J.: Bathymetry impacts on water exchange modelling through the Danish Straits, Journal of Marine Systems, 65(1-4), 450-459, doi:10.1016/j.jmarsys.2006.01.017, 2007

Sheldon, J.E., & Alber, M.: A comparison of residence time calculations using simple compartment models of the Altamaha River estuary, Georgia. Estuaries, 25 (6B), 1304-1317, doi:10.1007/BF02692226, 2002

5   Simonov, A. I., & Altman, E. N.: Hydrometeorology and Hydrochemistry of the USSR seas. Vol. 4. The Black Sea., St. Petersburg, Gidrometeoizdat (in Russian), 1991

Soto-Navarro, J., Somot, S., Sevault, F., Beuvier, J., Criado-Aldeanueva, F., Garca-Lafuente, J., Béranger, K.: Evaluation of regional ocean circulation models for the Mediterranean Sea at the Strait of Gibraltar: volume transport and thermohaline properties of the outflow, Climate Dynamics, 44, 1277-1292, doi: 10.1007/s00382-014-2179-4, 2015

10   Sozer, A, Ozsoy, E.: Modeling of the Bosphorus exchange flow dynamics, Ocean Dynamics, 67, 321–343, doi:10.1007/s10236-016-1026-z, 2017

Stanev, E. V.: On the mechanisms of the Black Sea circulation. Earth-Science Reviews, 28, 285-319, doi:10.1016/0012-8252(90)90052-W, 1990

Stanev, E. V., Grashorn, S., & Zhang, Y. J.: Cascading ocean basins: numerical simulations of the circulation and interbasin

15   exchange in the Azov-Black-Marmara-Mediterranean Seas system, Ocean Dynamics, 67, 1003-1025. doi:10.1007/s10236-017-1071-2, 2017

Stanev, E. V., & Staneva, J. V.: The impact of the baroclinic eddies and basin oscillations on the transitions between different quasi-stable states of the Black Sea circulation, Journal of Marine Systems, 24, 3-26. doi:10.1016/S0924-7963(99)00076-7, 2000

20   Staneva, J. V., Dietrich, D. E., Stanev, E. V., & Bowman, M. J. (2001), Rim Current and coastal eddy mechanisms in an eddy-resolving Black Sea general circulation model, Journal of Marine Systems, 31, 137–157. doi:10.1016/S0924-7963(01)00050-1, 2001

Wang, C. F., Hsu, M. H., & Kuo, A. Y.: Residence time of the Danshuei River estuary, Taiwan. Estuarine. Coastal and Shelf Science, 60(3), 381-393, doi:10.1016/j.ecss.2004.01.013, 2004

25   Woodgate, R. A., Aagaard, K., Weingartner, T. J.: Interannual changes in the Bering Strait fluxes of volume, heat and freshwater between 1991 and 2004, Geophysical Research Letters, 33, L15609, doi:10.1029/2006GL026931, 2006

Woodgate, R. A., Weingartner, T. J., Lindsay, R.: Observed increases in Bering Strait oceanic fluxes from the Pacific to the Arctic from 2001 to 2011 and their impacts on the Arctic Ocean water column, Geophysical Research Letters, 39(24), L24603, doi:10.1029/2012GL054092, 2012

30   Woodgate, R. A., Weingartner, T., Lindsay, R.: The 2007 Bering Strait oceanic heat flux and anomalous Arctic sea-ice retreat, Geophysical Research Letters, 37, L01602, doi:10.1029/2009GL041621, 2010

Xia, M., Xie, L., Pietrafesa, L.J.: Modeling of the Cape Fear River estuary plume, Estuaries and Coasts, 30, 698-709, doi:10.1007/BF02841966, 2007

Yankovsky, A. E., & Chapman, D. C.: A simple theory for the fate of buoyant coastal discharges, Journal of Physical Oceanography, 27, 1386-1401, doi:10.1175/1520-0485(1997)027<1386:ASTFTF>2.0.CO;2, 1997

Yuce, H.: Mediterranean water in the Strait of Istanbul (Bosphorus) and the Black Sea exit. Estuarine, Coastal and Shelf Science, 43(5), 597-616, doi.org/10.1006/ecss.1996.0090, 1996

5   Zatsepin, A. G., Ginzburg, A. I., Kostianoy, A. G., Kremenitskiy, V. V., Krivosheya, V. G., Stanichny, S. V., Poulain, P-M.: Observations of Black Sea mesoscale eddies and associated horizontal mixing, Journal of Geophysical Research, 108, 3246, doi:10.19/2002JC001390, 2003

Zavialov, P. O., Izhitskiy, A. S., & Sedakov, R. O.: Sea of Azov waters in the Black Sea: Do they enhance wind-driven flows on the shelf? In Velarde, M., Tarakanov, R., & Marchenko, A. (Eds.), The Ocean in Motion (pp. 461-474). Springer
10   Oceanography, Springer, Cham, doi:10.1007/978-3-319-71934-4_28, 2018
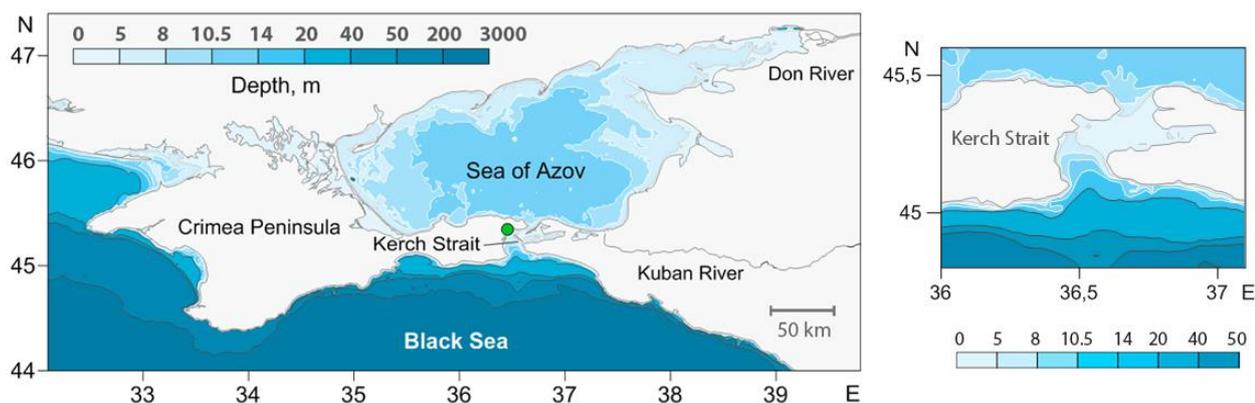
Figure 1: Bathymetry of the Sea of Azov and the northeastern part of the Black Sea (left) and the Kerch Strait (right). Locations of
15   **the estuaries of the Don and Kuban rivers and the Kerch meteorological station (green circle).**
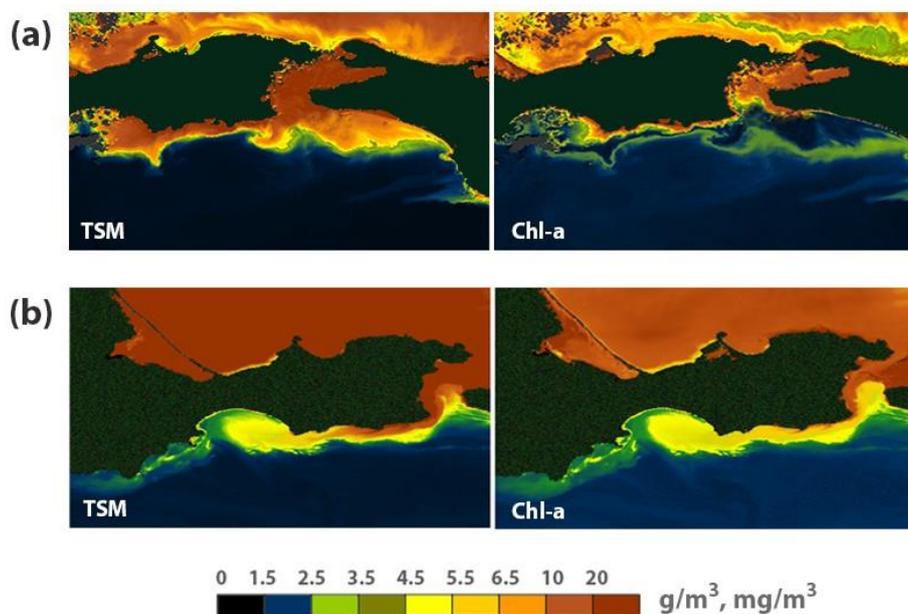
Figure 2: Sea surface distributions of TSM (left) and Chl-a (right) retrieved from MERIS satellite data indicating wind-induced resuspension of sea bottom sediments at the study area on 2 April 2012 (a) and spreading of AP on 20 April 2004 (b).
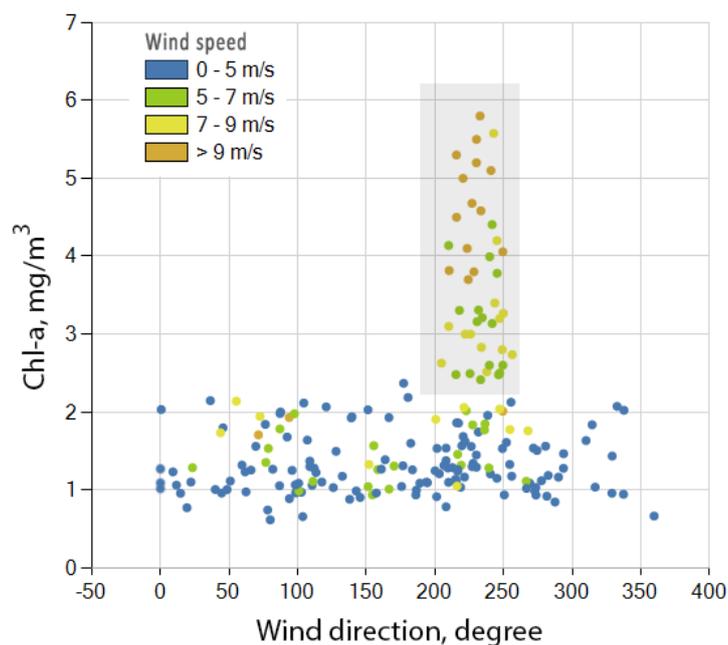
5

Figure 3: Dependence between concentration of Chl-a in the Kerch Strait and the adjacent area of the Black Sea retrieved from optical satellite imagery, on the one hand, and direction of wind forcing averaged over 24 hours preceding satellite observations, on the other hand.
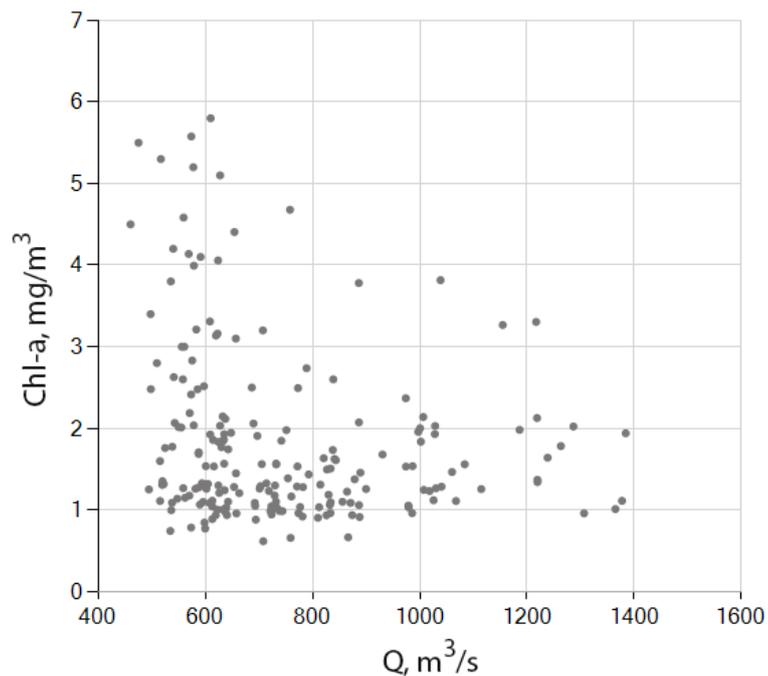
Figure 4: Dependence between concentration of Chl-a in the Kerch Strait and the adjacent area of the Black Sea retrieved from optical satellite imagery, on the one hand, and total discharge of the Don and Kuban rivers, on the other hand.
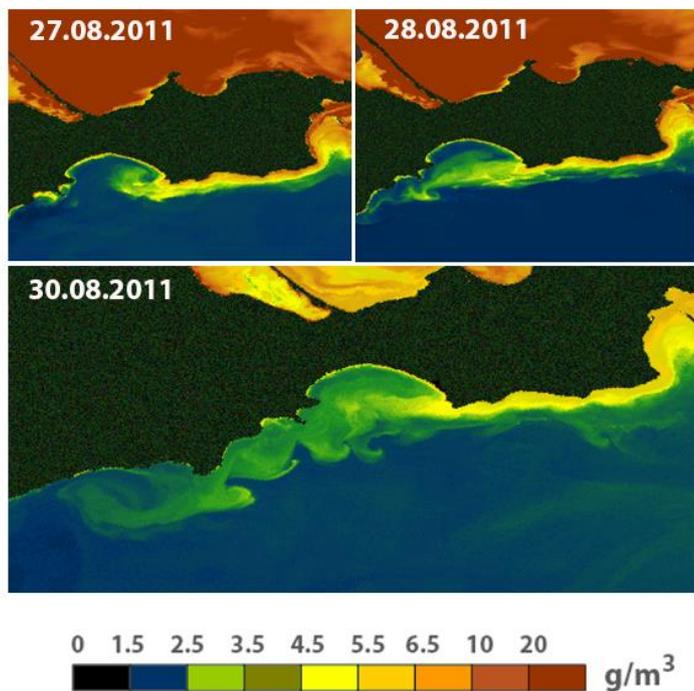
Figure 5: Temporal variability of AP identified at satellite surface distributions of TSM on 27, 28, and 30 August 2011 retrieved from MERIS satellite data.

Ocean Science
Discussions
Open Access
EGU
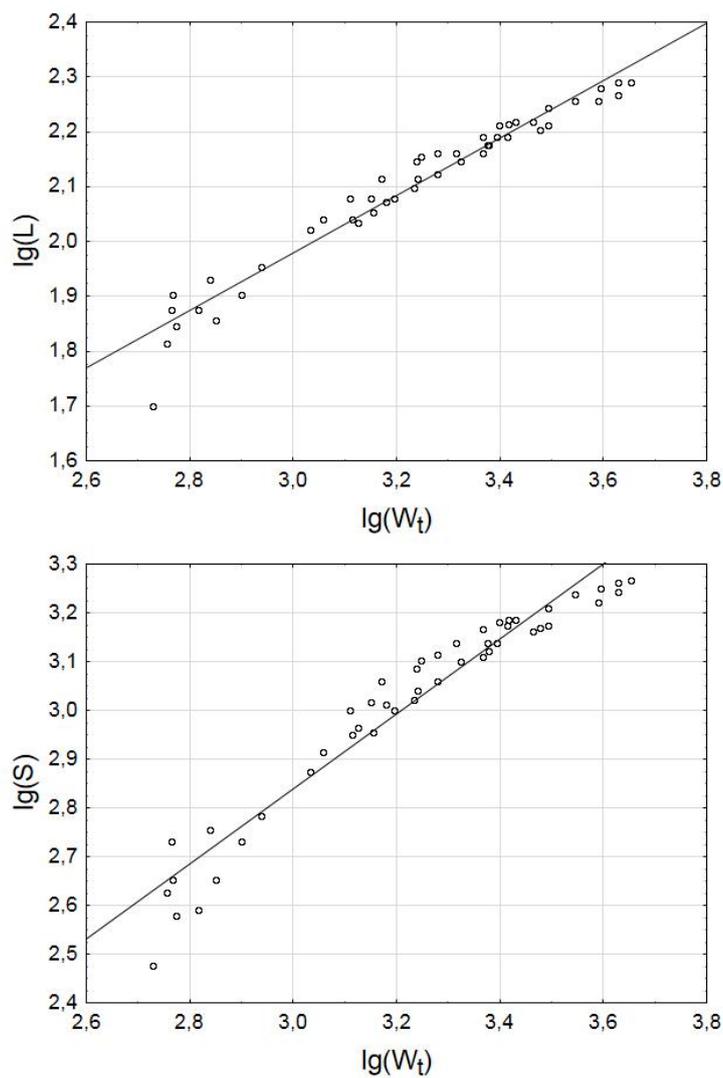
Figure 6: Dependence between alongshore extent of AP (top) and area of AP (bottom) calculated from satellite data, on the one hand, and wind forcing index for the period of predominant northeastern winds preceding time of satellite observations, on the other hand.

5
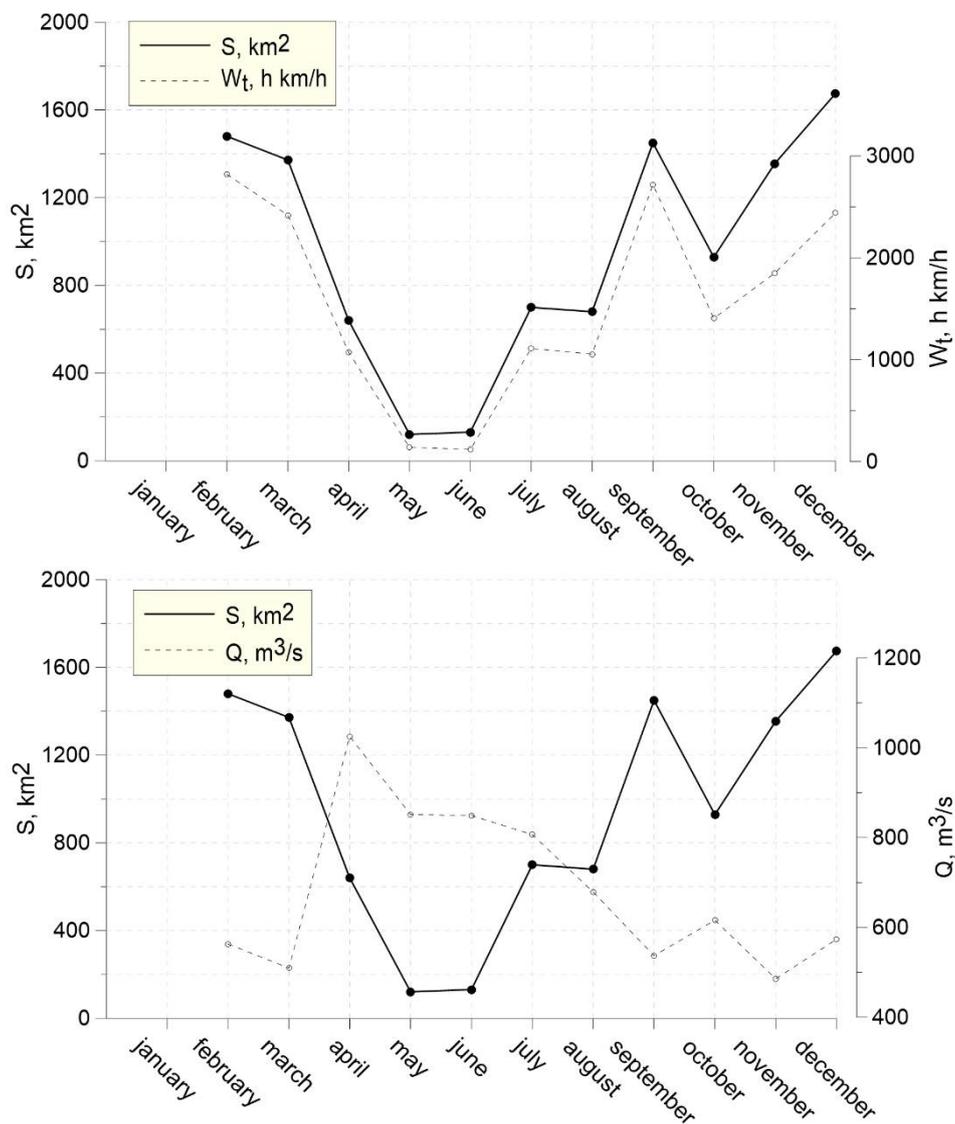
Figure 7: Dependence between monthly averages of wind index (top) and total discharge rate of the Don and Kuban rivers (bottom), on the one hand, and monthly averages of area of AP detected at optical satellite imagery, on the other hand.

Ocean Science

Discussions

Open Access
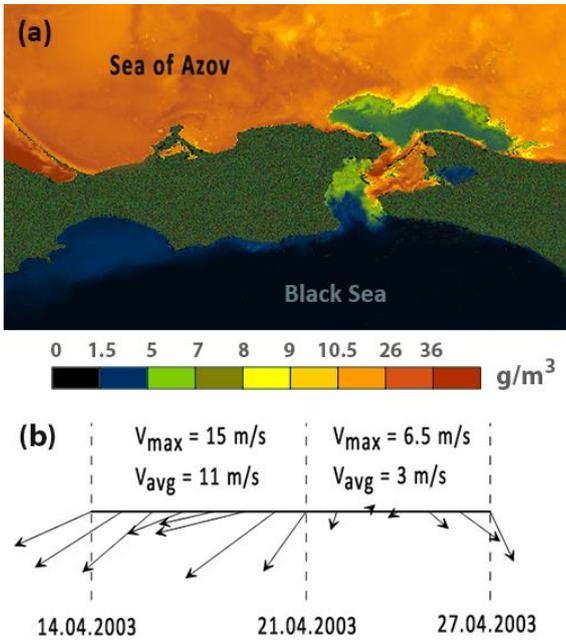
Figure 8: BP formed during 21-27 April 2003 and AP formed during 14-21 April 2003 identified at satellite surface distributions of TSM on 27 April 2003 retrieved from MERIS satellite data (a); local wind forcing with indication of its maximal and average values during 14-21 and 21-27 April 2003 (b).

5
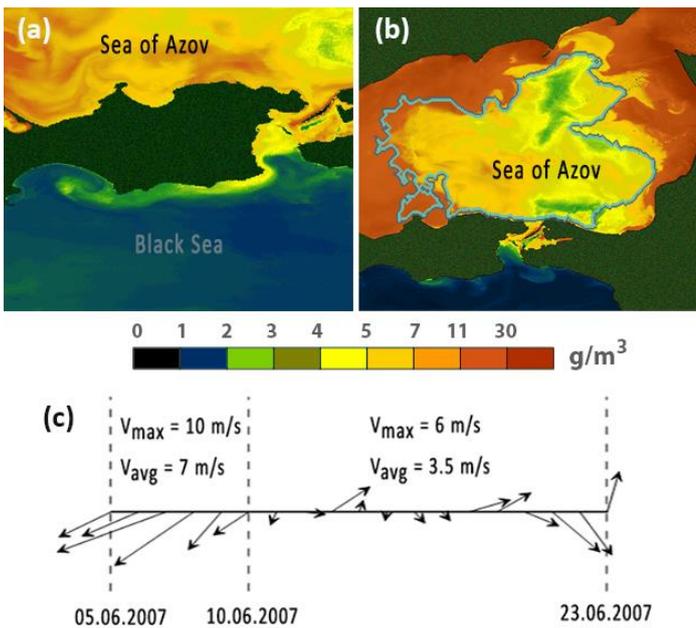
Figure 9: AP on 6 June 2007 (a) and BP on 23 June 2007 (b) identified at satellite surface distributions of TSM retrieved from MERIS satellite data; local wind forcing with indication of its maximal and average values during 5-10 and 10-23 June 2007 (c). The isobath of 10 m of the Sea of Azov is indicated by the blue line (b).

Ocean Science
Discussions
Open Access
EGU

Table 1: Mean monthly and annual frequency, duration, share of AI-favorable and BI-favorable wind conditions and discharge volume from the Sea of Azov to the Black Sea estimated during the period of 2000-2017.

	Mean frequency of AI-favorable wind conditions	Mean duration of AI-favorable wind conditions, hours	Share of AI-favorable wind conditions, %	Mean frequency of BI-favorable wind conditions	Mean duration of BI-favorable wind conditions, hours	Share of BI-favorable wind conditions, %	Discharge volume from the Sea of Azov to the Black Sea, km^3
January	2.2	117.5	35	2.1	248.6	65	5.68
February	2.4	117.2	39	2.3	165.2	61	5.38
March	2.1	99.6	30	2.0	268.0	70	4.56
April	2.1	95.3	28	2.1	244.4	72	4.05
May	1.2	92.5	15	1.3	545.1	85	3.66
June	0.9	91.4	11	0.8	718.5	89	3.54
July	1.1	98.4	15	1.0	640.0	85	4.02
August	1.7	102.0	25	1.6	354.2	75	4.07
September	2.4	108.0	36	2.1	223.5	64	4.46
October	3.1	119.1	52	2.8	135.0	48	5.45
November	2.4	108.0	36	2.3	203.7	64	4.58
December	2.7	96.9	37	2.5	195.2	63	4.32
Year	24.3	103.8	29	22.9	328.5	71	53.69

5